Dynamic holographic interferometry using a $Bi_{12}SiO_{20}$ photorefractive crystal and monomode optical fibres

J. Potter[1], R. C. Spooncer[1] and P. R. Hobson[2]

[1]The Brunel Centre for Manufacturing Metrology, Brunel University, Uxbridge, Middlesex UB8 3PH, UK,
[2]The Department of Physics, Brunel University, Uxbridge, Middlesex UB8 3PH, UK.

ABSTRACT

Dynamic holographic interferometry using polarization preserving optical fibres as light guides and incorporating a photorefractive $Bi_{12}SiO_{20}$ (BSO) crystal as the recording medium is described. An experimental investigation of the recording of time average holograms through the diffusion process (employing anisotropic self-diffraction) and the drift process (application of d.c. and a.c. electric fields across the crystal) is also described. The holographic interferometer was optimised to produce holograms with a high diffraction efficiency and a high signal-to-noise ratio. Results are presented on optimising parameters such as the writing beam angle and writing beam intensity ratio. The advantages that can be gained by deploying this holographic interferometer in an industrial environment, where the laser light is guided to the location of the object by means of monomode fibres and images are stored within a photorefractive crystal is described. The holographic interferometer is capable of producing time average and double exposure interferograms of vibrating and deformed objects which can be displayed in real time.

1. INTRODUCTION

1.1. The photorefractive effect

The photorefractive effect was first observed in 1966[1] occurring in poled single crystals of potassium tantalate niobate (KTN). The effect was caused by illuminating the crystal with a laser beam of several milliwatts and the effect became physically evident when the crystal was probed with a second beam. The photorefractive effect causes a change in the refractive index and the effect has been observed in a number of materials such as ferroelectric, sillenite and semiconductor crystals, ferroelectric ceramics, organic crystals and organic polymers. Initially the index change was viewed as optical damage and research was conducted towards eliminating this damage, which was seen to have a detrimental effect on the optics of nonlinear devices. This concern led to the discovery that the optical damage could be reversed by illuminating the crystal with a laser beam with a spot size equal or larger than the damaged area and with a wavelength similar to the light that caused the original damage[2]. The photorefractive process is now well understood and the process can be explained by considering a sinusoidal interference pattern incident on an electro-optic crystal as in figure 1a. The incident nonuniform illumination causes charge carriers, in the form of electrons and holes, to be excited from impurity or defect sites within the crystal. The charge carriers are transported from the brightly illuminated regions to darker regions of the crystal. The transport of charge carriers can be influenced by three different mechanisms: diffusion; drift and the photovoltaic effect, any one of the mechanisms may dominate the transport process. The space charge field within the crystal is modulated due to the separation of charges. A phase shift between the electric space charge field within the crystal and the incident interference pattern results, as shown in figure 1b. In BSO the photovoltaic effect does not contribute to the transport of carriers and if no applied electric field is present the movement of carriers is influenced by diffusion alone. In the diffusion process the phase shift is exactly 90°[3].

 0-8194-0905-7/93/$4.00

The electric space charge field causes a refractive index grating to be created via the electro-optic Pockels effect, as shown in figure 1c.

Figure 1 The Photorefractive effect

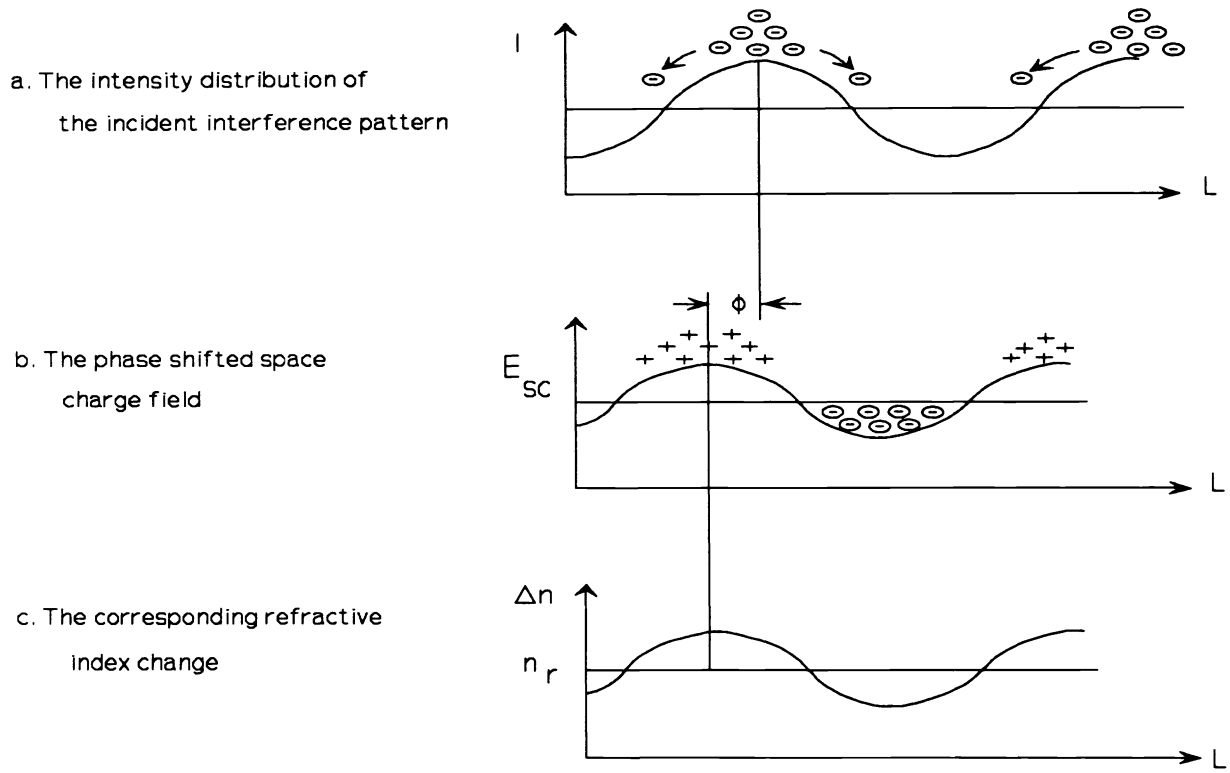

The photorefractive effect was first utilised in holographic recording in 1968[4] and has provoked considerable interest ever since. The photorefractive crystal when used as a holographic recording media has the advantage over conventional silver halide plates in that no processing or developing is required and the crystal can be erased and reused. The sensitivity of the BSO crystal is comparable to silver halide plates and gratings can be recorded in the crystal at power levels as low as 50 μWcm^{-2} when using laser light of wavelength 514.5 nm.

1.2 Holography with monomode optical fibres

The usual function of optical components that are used in conventional holography systems can also be accomplished by using optical fibres[5,6]. A fibre optic holography system eliminates several problems that are found in conventional systems to be over come and in addition provides a number of distinct advantages. The advantages are listed below.

- The laser can be placed in a remote area away from the exposed object area
- The object is isolated from the acoustic noise of the laser
- Potentially hazardous open laser beams are avoided in the work area
- The number of optical components within the system is reduced as spatial filtered beams are produced by the fibres
- Flexible optical fibres allow access to areas of an object where no direct line of sight exists
- High birefringent monomode fibres have a relative insensitivity to environmental perturbations without the consequent polarization scrambling that occurs in conventional monomode fibre

The fibre holography system used in the following experiments is a commercially available system[7] which consists of a launch head and two flexible steel armoured high birefringent 'bow tie' monomode fibres which deliver the object and reference beams. The launch head which consists of a polarisation preserving beam splitting cube and half wave plate which provides the beam splitting ratio to be varied between 1 and 99%. The launch head is placed in front of the laser aperture and simple two axis angular adjustments are made in order to achieve the transmission of laser power through the fibres. The two laser beams emerging from the beam splitter are focused onto the core of each fibre via pre-aligned lenses which are connected to the input end of each fibre.

2. THE HOLOGRAPHIC INTERFEROMETER CONFIGURATION

Figure 2 is a schematic diagram of the fibre optic holographic interferometer. The launch head containing the beam splitter is manufactured such that optimum operation is achieved with the laser beam aligned to the centre of the input aperture of the waveplate holder and the centre of the output apertures of the two cylindrical turrets in which the optical fibres are placed. In order to achieve this the launch head was adjusted for both spatial and angular orientation and the laser beam was centred to better than $\pm$ 0.5 mm at the three apertures. Both the laser and the launch head were mounted on a specially designed frame in order to meet the mechanical positioning tolerance. The fibres were then placed in the turrets and the four positioning screws and two tension screws within each of the turrets were carefully adjusted until the transmission of laser light was observed at the output end of each fibre. The birefringent axes of each fibre is marked on both the input and output ferrule at the end of each fibre. A polarizer was placed close to the output end of each fibre such that the fast axis of the polarizer was orthogonal to the cross hair birefringent axes marking on the output ferrule of the fibre. Thus the transmitted laser light was virtually extinguished by the polarizer. The input ferrule of the fibre was rotated in the turret until complete extinction occurred, the residual light transmitted through the polariser was monitored with a photodiode.

A fibre ferrule holder allows the output fibre to be rotated and the birefringent axes of the fibre to be preset to a specified angle with respect to the vertical axes of the holder which is orthogonal to the surface of the optical table. Thus both fibres can be set such that the angle of the plane of polarization of the emerging light can be determined. The polarisation angle is measured with a protractor that is attached to the back of each of the fibre ferrule holding units. The ferrule holding units contain a lens mounting which can be easily positioned to produce a collimated beam. High birefringence fibres are available with a lens connected to the fibre end which produce a collimated beam with a pre-defined diameter.

Figure 2 The holographic interferometer configuration

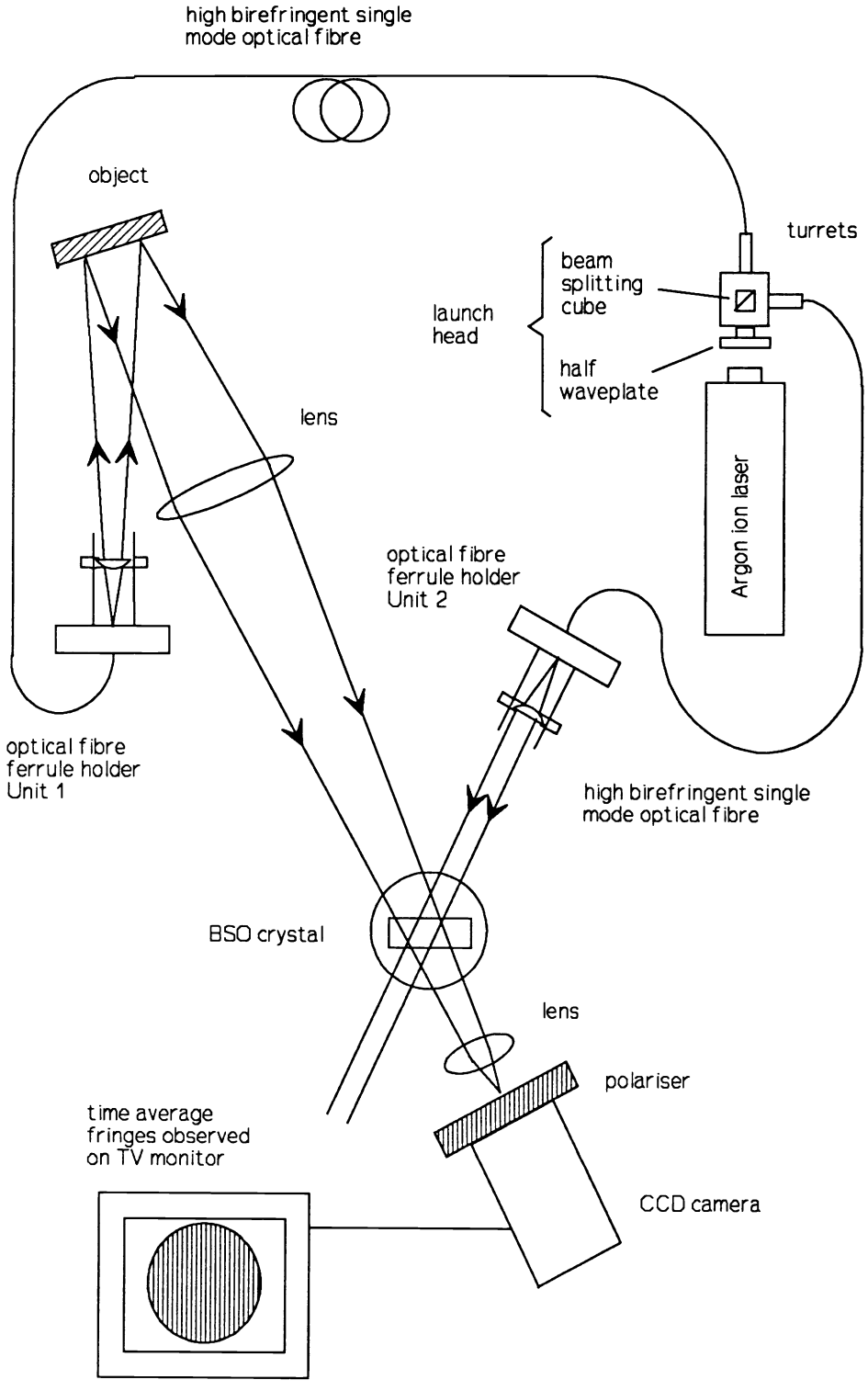

The majority of experimental work was aimed at determining the optimum recording parameters for real time holographic interferometry. The experiments were performed using the system shown in figure 1. However, the object was replaced by a mirror, the CCD camera was replaced by a photodetector and the object and reference beams were collimated to produce a 4 mm diameter beam that was incident on the BSO crystal.

3. ANISOTROPIC SELF-DIFFRACTION IN BSO

The design of the holographic interferometer is based on the phenomena of anisotropic self diffraction. In the configuration shown in figure 2 the reference and object beams interfere at the location of the crystal and a phase volume holographic grating is created within the crystal due to the photorefractive effect. The grating stored in the crystal causes the reference beam to be diffracted into the path of the transmitted object beam. The anisotropic self diffraction that occurs in BSO produces a rotation in linear polarization of the diffracted reference beam with respect to the transmitted object beam.

Two alternative crystal orientations have been used for volume holography, in both orientations the crystal is cut to expose the (11bar0), the (110), and the (001) crystallographic faces[8]. In the crystal configuration used in this work the (001) axis was perpendicular to the holographic grating vector K_G. The maximum phase grating amplitude has been shown to occur for this orientation when the linearly polarised incident light is incident along and perpendicular to an axis bisecting the [001] and [110] crystal axes as shown in figure 3[9].

Figure 3 Crystal orientation and incident linear polarized writing beams used to produce a maximum phase grating amplitude

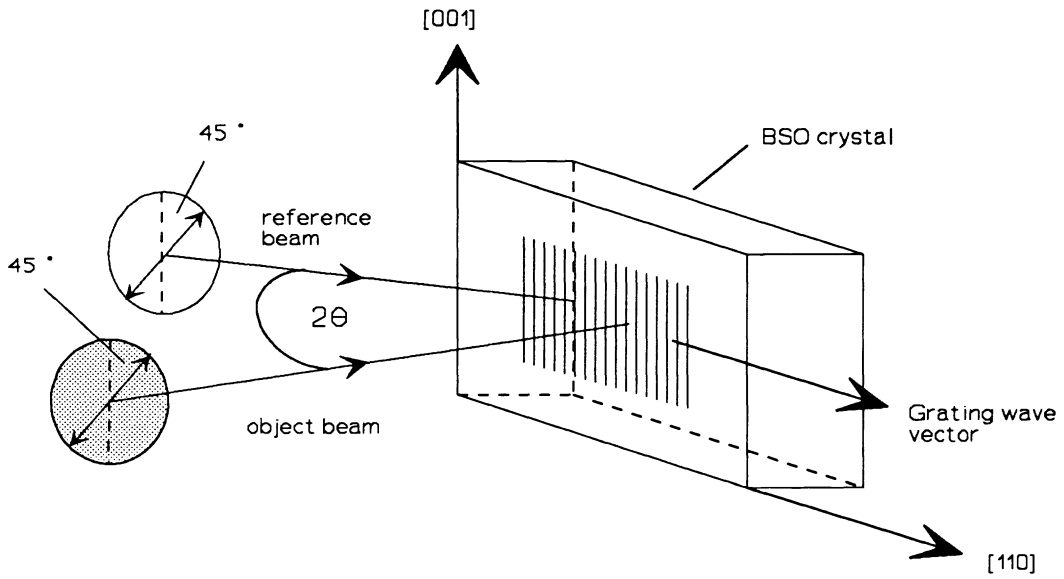

In diffusion recording the shifted phase gratings produced by the writing beam polarisations shown in figure 3 are of opposite signs. This causes the writing beam polarisations to be rotated and in the case of a crystal possessing no optical activity the crystal acts as a half wave plate. The diffracted reference beam polarization is rotated with respect to the transmitted object beam. However, BSO which is a body centred cubic crystal that exhibits point group symmetry 23 and is optically active. A maximum polarization separation of 90° between the self diffracted reference beam and the transmitted object beam polarizations has been shown to be obtained when the reference beam polarisation is parallel to the [001] axis at the centre of the crystal when optical activity is present[10]. The BSO crystal used in this work was 3mm thick and possessed optical activity that was determined to be 39°/mm at 514.5 nm. Ideally in order to produce both a phase grating with a maximum amplitude and a maximum polarization separation of 90° between the self diffracted and transmitted beam polarizations in a BSO crystal with optical activity of 39°/mm the thickness of the crystal should be ≈ 2.3 mm. When the maximum polarization separation of 90° is produced the transmitted object beam which can be regarded as the noise of the image can be cancelled by a linear polarizer leaving the diffracted reference beam and thus an increased signal to noise ratio of the image. The linear polariser that was used to cancel the transmitted object beam was an HN22 sheet polarizer and was placed on the opposite side of the crystal with respect to the writing beams as shown in figure 2.

4. OPTIMISING THE WRITING BEAM PARAMETERS

The writing parameters that require optimising are the writing beam angle, 2θ, and the writing beam intensity ratio, ß. The writing beam intensity ratio is defined at the ratio of the intensity of the object beam to the intensity of the reference beam. The experimental procedure involved setting the writing beam intensity ratio equal to one and measuring the corresponding diffraction efficiency, η, for various writing beam angles. In order to calculate the diffraction efficiency which is defined as the percentage of the incident reference beam that is diffracted by the stored grating the incident reference beam and diffracted reference beam intensities were measured with a photodetector. Measurement of the object beam intensity was also required in order to determine the writing beam intensity ratio. The diffraction efficiency as a function of the writing beam angle is shown in figure 4, the diffraction efficiency was measured for two different laser power levels. The optimum writing beam angle was determined to be ≈ 44°. With the writing beams set at the optimum writing beam angle the diffraction efficiency was then measured as a function of the writing beam intensity ratio, the results are shown in figure 5. The diffraction efficiencies observed in the above experiments where recording is carried out in the diffusion regime (i.e. no electric fields are applied) is of the same order of magnitude as the wavefront reflectivity observed in a four wave mixing phase conjugate configuration that incorporates BSO as the recording media[11].

The graph of the diffraction efficiency as a function of the writing beam intensity ratio shown in figure 5 indicates that the maximum diffraction efficiency is observed at ß ≈ 1 a condition which is also observed in holography experiments with silver halide photographic plates.

Although the diffracted light measured when the grating was written with a higher writing beam intensity (as in figure 5) was higher compared to the diffracted light from the grating that was written with a lower writing beam intensity (as in figure 4) the diffraction efficiency which is a measure of the diffracted light as a percentage of the reference beam intensity was observed to decrease slightly.

Figure 4 The diffraction efficiency, η, as a function of the writing beam angle, 2θ.

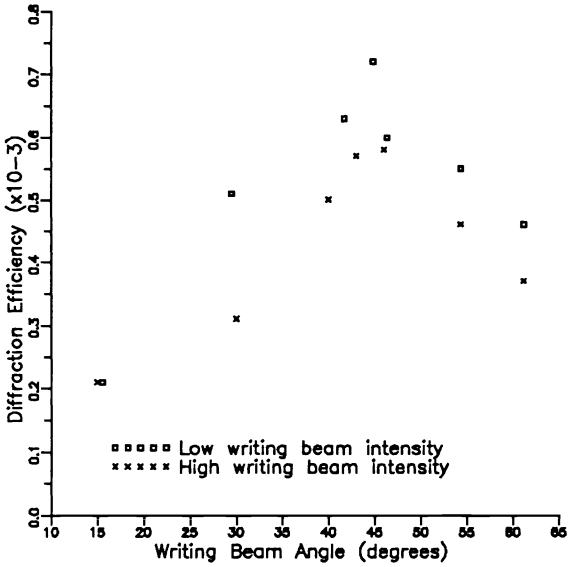

Figure 5 The diffraction efficiency, η, as a function of the writing beam intensity ratio, ß.

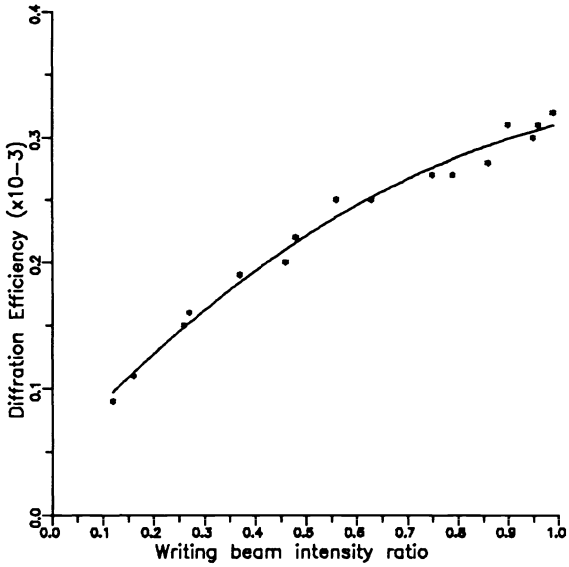

This can be explained by considering the recording and erasure cycle of the grating. The formation time of the grating which is defined in this work as the time taken for the grating to increase from 10% to 90% of the saturation level, was measured and found to be longer than the erasure time, which is defined in a similar manner. The formation and erasure times are shown as a function of the writing beam angle in figure 6. The explanation for the decrease in the diffraction efficiency for increasing writing beam intensities can be explained as follows:-

The grating increases until saturation is reached and no increase in the diffracted light intensity is observed. In the holographic interferometer configuration shown in figure 2 both writing beams are continuously incident upon the crystal. When the grating reaches the saturation level the grating is simultaneously both erased and re-formed. As shown in figure 6 the erasure time is faster than the formation time which results in a net reduction in the grating strength. The grating is erased by the reference beam and the higher the intensity of the reference beam the more the grating is erased. The reduced grating strength results in a lower diffraction efficiency being observed.

The highest diffraction efficiency is observed at an angle $\approx 44°$ and when the writing beam intensity ratio, ß, equals one. However, the intensity of the residual object beam transmitted through the polarizer is higher at ß=1 than the residual transmitted object beam at ß<1.

Thus the signal to noise ratio of the holographic image is lower at ß=1 than at ß<1. In figure 7 the image to background intensity ratio (IBR), which is defined as the ratio of the diffracted reference beam intensity to the transmitted object beam intensity[12], is plotted as a function of the writing beam intensity ratio, ß. The maximum IBR is observed at ß ≈ 0.27 and the diffracted reference beam intensity is 65 times the residual transmitted object beam. At ß = 1 the diffracted reference beam is only 43 times the intensity of the transmitted object beam. A compromise is therefore required between a high diffraction efficiency and a high IBR. Despite the reduced diffraction efficiency that results from the above compromise the diffraction efficiency obtained is adequate for imaging the object image on a TV monitor with the aid of a CCD camera. With the writing beam parameters optimised time average interferograms of an aluminium surface coated glass plate were produced.

Figure 6 The grating formation and erasure times as a function of the writing beam angle, 2θ.

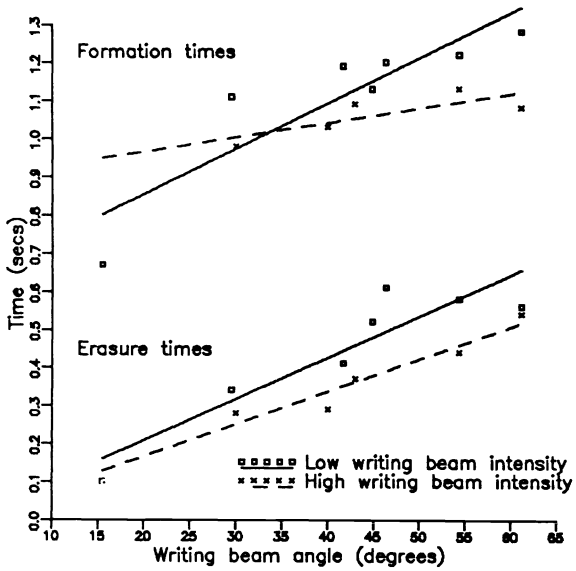

Figure 7 The Image to Background intensity Ratio as a function of the writing beam intensity ratio, ß.

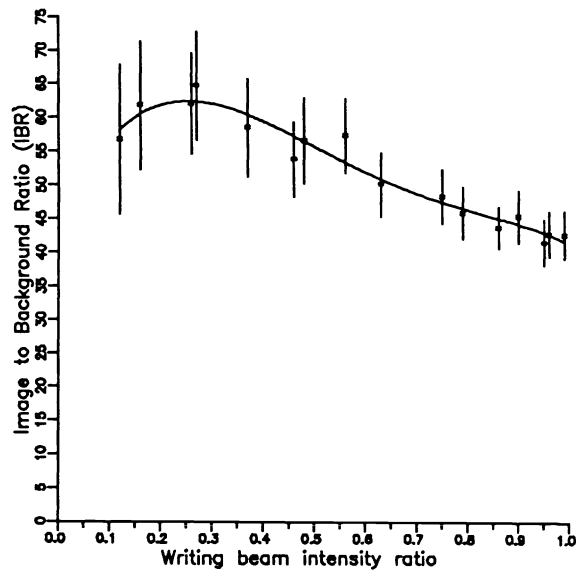

5. OBTAINING TIME AVERAGE INTERFEROGRAMS

The glass plate was mounted in front of a speaker which was connected to an audio amplifier and sound from the speaker was successfully coupled to the glass plate. The reference beam was initially blocked and the object beam transmitted through the polarizer was imaged onto the CCD camera shown in figure 2.

The polarizer was then rotated in order to cancel the object beam and the then the reference beam was unblocked. In figure 8 a photograph of the time average interference fringes of the glass plate vibrating at a frequency of 450 Hz is shown. The image was obtained by photographing the time average image displayed on the TV monitor. The diameter of the illuminated object was 38 mm. The intensity of the object and reference beams incident on the crystal were 85 $\mu W/cm^2$ and 200 $\mu W/cm^2$ respectively ($\beta \approx 0.43$). The frequency of vibration was varied and a new image was formed in approximately two seconds. The formation and erasure time of the grating was measured for different writing beam intensity ratios and the results are shown in figure 9. The erasure time was found to be faster than the formation time as in figure 6, both the formation and erasure times were seen to increase as the writing beam intensity ratio decreased.

Figure 8 Time average interferogram of a vibrating aluminum coated glass plate vibrating at a frequency of 450 Hz

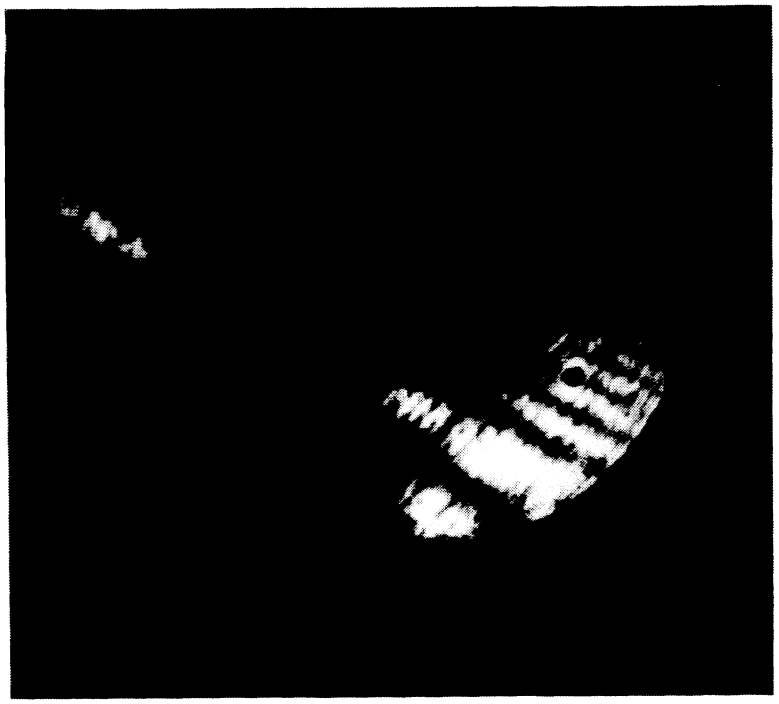

6. CONCLUSION

The anisotropic self diffraction properties of BSO have been utilised to produce time average interferograms with a high contrast and high resolution similar to that obtained in photographic plate holography. The fibre holography system described above is capable of producing interferograms in real time within a recording media that can be used many times. The use of monomode optical fibres to supply both the reference and object beams provides many additional advantages which have been described above.

Figure 9 The grating formation and erasure times as a function of the writing beam intensity ratio, ß.

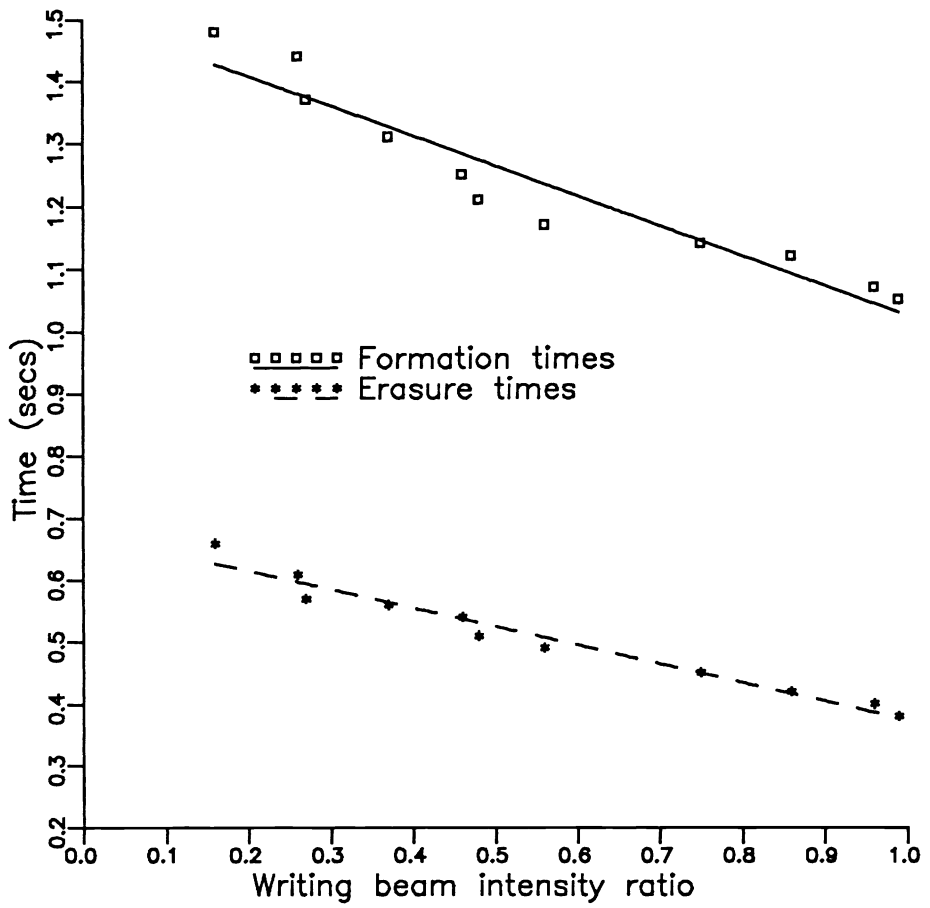

The requirement of a large writing beam angle gives a distinct advantage over four wave mixing configurations in that the object can be placed relatively close to the crystal which allows interferograms of diffusely reflecting objects can be more easily obtained. The fibre holography system is also much simpler as the fibres automatically produce spatially filtered beams and no applied electric fields are required. However, careful attention must be paid to optimising the recording parameters. In the near future an investigation into the application of both d.c. and a.c. electric fields across the crystal will be undertaken. Such fields have been shown to cause a dramatic increase in the diffraction efficiency, diffraction efficiencies of up to 25% have been observed with an applied d.c. field of 9 kV/cm.[13] The application of electric fields with the corresponding increase in the diffraction efficiency will allow some relaxation in how carefully the writing parameters must be optimised. A fibre holography system with applied electric fields should prove to be more adaptable to an industrial environment when the requirement of the careful optimisation of the system can be avoided.

7. ACKNOWLEDGEMENTS

The authors gratefully acknowledge the assistance of Dr. D. C. Williams of the Division of Mechanical and Optical Metrology at the National Physical Laboratory, Teddington, Middlesex, and Mr. Roger Troth of the Applied Optics Section, Blackett Laboratory, Imperial College, London, and the financial support provided by the Science and Engineering Research Council and the National Physical Laboratory.

8. REFERENCES

1. F. S. Chen, J. E. Geusic, S. K. Kurtz, J. G. Skinner and S. H. Wemple, "Light Modulation and Beam Deflection with Potassium Tantalate-Niobate Crystals," J. Appl. Phys. vol 37, no. 1, pp. 388-398, Jan. 1966.

2. A. Ashkin, G. D. Boyd, J. M. Dziedzic, R. G. Smith, A. A. Ballman, J. J. Levinstein and K. Nassau, "Optically-induced refractive index homogeneities in $LiNbO_3$ and $LiTaO_3$," Appl. Phys. Letts. vol 9, no. 1, pp. 72-74, July 1966.

3. L. Young, W. K. Y. Wong, M. L. W. Thewalt and W. D. Cornish, "Theory of formation of phase holograms in lithium niobate," Appl. Phys. Letts. vol 24, no. 6, pp 264-265, March 1974.

4. F. S. Chen, J. T. LaMacchia and D. B. Fraser, "Holographic Storage in Lithium Niobate," Appl. Phys. Letts. vol 13, no. 7, pp. 223-225, Oct. 1968.

5. A. M. P. P. Leite, "Optical fibre illuminators for holography," Opt. Commun. vol 28, no. 3, pp. 303-308, March 1979.

6. J. D. C. Jones, M. Corke, A. D. Kersey and D. A. Jackson, "Single-mode fibre optic holography," J. Phys. E:Sci. Instrum. vol 17, pp. 271-273, 1984.

7. The fibre holography system is manufactured by York V.S.O.P. Ltd, School Lane, Chandlers Ford, Hampshire SO5 3DG, UK, 1990.

8. A. Marrakchi, J. P. Huignard and P. Gunter, "Diffraction Efficiency and Energy Transfer in Two-Wave Mixing Experiments with $Bi_{12}SiO_{20}$ Crystals," Appl. Phys. vol 24, pp. 131-138, 1981.

9. M. P. Petrov, T. G. Pencheva and S. I. Stepanov, "Light diffraction from volume phase holograms in electrooptic photorefractive crystals," J. Optics (Paris). vol 12, no. 5, pp. 287-292, 1981.

10. A. Marrakchi, R. V. Johnson and A. R. Tanguay, Jr, "Polarisation properties of photorefractive diffraction in electrooptic and optically active sillenite crystals (Bragg regime)," J. Opt. Soc. Am. B. vol 3, no. 2, pp. 321-336, Feb. 1986.

11. J. P. Huignard, J. P. Herriau, G. Rivet and P. Gunter, "Phase-conjugation and spatial-frequency dependence of wave-front reflectivity in $Bi_{12}SiO_{20}$ crystals," Opt. Letts. vol 5, no. 3, pp. 102-104, March 1980.

12. R. C. Troth and J. C. Dainty, "Holographic interferometry using anisotropic self-diffraction in $Bi_{12}SiO_{20}$," Opt. Letts. vol 16, no. 1, pp. 53-55, Jan. 1991.

13. J. P. Huignard and F. Micheron, "High-sensitivity read-write volume holographic storage in $Bi_{12}SiO_{20}$ and $Bi_{12}GeO_{20}$ crystals," vol 29, no. 9, pp. 591-593, Nov. 1976.